Universiteit Utrecht

Fifteenth Meeting of the Benelux EPR Group

Programme
Book of Abstracts
List of participants

April 20, 2007

Minnaert building,
Leuvenlaan 4, De Uithof, Utrecht.

15th Meeting of the Benelux EPR Group 2007

Utrecht – April 20

Registration and venue site: room 211, Minnaert building
Leuvenlaan 4
De Uithof, Utrecht

10:00 Registration and coffee/tea

10:30 Welcome by Ernst van Faassen

10:35 CW- and Pulsed EPR study of transition-metal doped porous catalysts
Sepideh Zamani, Sabine Van Doorslaer, Alina-Mihaela Hanu, Evi Beyers, Vera Meynen, Pegie Cool, Etienne Vansant (Antwerp, B)

11:00 Spectroscopic and redox properties of Nar1, a protein involved in biological iron-sulfur cluster biosynthesis
Peter-Leon Hagedoorn, G. Paul H. van Heusden, H. Yde Steensma, Wilfred R. Hagen (Delft, NL)

11:25 Inherent point defects in tensile strained (100)Si/SiO_2 entities probed by electron spin resonance.
P. Somers, V. V. Afanas'ev, and A. Stesmans (Leuven, B)

11:50 High resolution 2D and 3D EPR molecular imaging of melanin in melanomas.
E.S. Vanea, N. Charlier, M. Dinguizli, J. Dewever, O. Feron, B. Gallez (Louvain, B)

12:15 LUNCH

14:15 The distance between a native cofactor and a spin label by a two -frequency pulsed electron paramagnetic resonance method (DEER)
Igor V. Borovykh, Stefano Ceola, Prasad Gajula, Sergey Milikisyants, Peter Gast, Heinz-Jürgen Steinhoff, Martina Huber (Leiden, NL)

14:40 EPR and ENDOR investigation of the positive polaron in the doped polymers MDMO-PPV and P3HT
A. Aguirre , G. Janssen, E. Goovaerts, S. Van Doorslaer, S. Orlinski , E. Groenen (Antwerp, B)

15:05 Enhanced release of nitric oxide from endothelial cells under anoxia.
Ernst van Faassen (Utrecht, NL)

15.30 General discussion

15.40 Poster session and Tea
Drinks

17.00 Poster Awards

18.00 End

ABSTRACTS

Oral presentations

CW- and Pulsed EPR study of transition-metal doped porous catalysts

Sepideh Zamani[1], Sabine Van Doorslaer[1], Alina-Mihaela Hanu[2], Evi Beyers[3], Vera Meynen[3], Pegie Cool[3], Etienne Vansant[3]

[1] *University of Antwerp, Department of Physics, Universiteitsplein 1, 2610 Wilrijk, Belgium*

[2] *"Al. I. Cuza" University of Iasi, Department of Physical and Theoretical Chemistry and Materials Chemistry, Bvd. Carol I, no 11, 700506, Romania*

[3] *University of Antwerp, Department of Chemistry, Universiteitsplein 1, 2610 Wilrijk, Belgium.*

This work focuses on the analysis of two types of porous materials based on silica and titanium dioxide respectively.

Since 1992, a wide variety of mesoporous materials (siliceous and non-siliceous) have gained growing interest, in order to overcome the limits in accessibility and applicability encountered for microporous zeolites. In this work, the hexagonal MCM-41 is studied. MCM-41 is characterized by a high surface area, narrow pore size distribution and larger pore sizes than the microporous zeolites. One of the biggest challenges is the embedding of the metal sites (the actual catalytic sites) into the porous structure rather than depositing it on the support walls. In the first part of this work, we present an electron paramagnetic resonance (EPR) study of the incorporation of vanadium in MCM-41 via different chemical routes. We compare vanadium deposition in the pores via the molecular designed dispersion (MDD) method with a facile, direct room-temperature synthesis targeted at vanadium incorporation into the MCM-41 framework. The difference between the two routes is monitored by studying the vanadyl-containing precursors of the final catalysts. It will be shown how important information about the mobility and incorporation mechanism of the vanadyl species in the mesoporous systems can be revealed by the use of X-band continuous-wave and 2-dimensional pulsed EPR spectroscopy, such as HYSCORE.

Furthermore, semiconductor titanium dioxide (TiO_2) materials have been investigated over the last three decades due to their photocatalytic activities. The morphology and high surface areas of these materials are responsible for their high efficiency in catalysis. Some of the applications of these materials are, self-cleaning building materials, solar sells, etc. Here, H-tube materials (tube-like TiO_2) are doped with different transition metals, such as vanadium and copper ions, using the MDD method. The doping is targeted at improving the catalytic properties of the material and at the reduction of the band gap, which lies in the UV range for the undoped material. In the second part of this work, we will focus on the EPR study of these materials at different temperatures under UV and visible light irradiation. In this way, information about the photo-induced charge separation is obtained.

Spectroscopic and redox properties of Nar1, a protein involved in biological iron-sulfur cluster biosynthesis

Peter-Leon Hagedoorn[1], G. Paul H. van Heusden[2], H. Yde Steensma[2] and Wilfred R. Hagen[1]

[1]*Department of Biotechnology, Delft University of Technology, Delft, The Netherlands*
[2]*Institute of Biology Leiden, Leiden University, Leiden, The Netherlands*

Nar1 from *Saccharomyces cerevisiae* (baker's yeast) has recently been found to be involved in biological iron-sulfur cluster biosynthesis (1). The precise role and mechanism of action of Nar1 remains a mystery. The protein shares significant homology with Fe-hydrogenase, a hydrogen producing and consuming enzyme found in anaerobic bacteria and unicellular eukaryotes (2). The catalytic site of Fe-hydrogenase is a unique iron-sulfur cluster with organometallic CO and CN ligands that has been named the H-cluster. The homology between Nar1 and Fe-hydrogenase indicates that all amino-acids that coordinate the H-cluster are conserved. Nar1 itself is an iron-sulfur cluster containing protein. Redox potentiometric titrations of Nar1 showed that the protein contains three redox active species: mononuclear iron, [3Fe-4S] cluster and [4Fe-4S] cluster. Strikingly the EPR signal of the $[3Fe\text{-}4S]^{+}$ cluster disappears abruptly above + 50 mV. This is indicative of instability of the iron-sulfur clusters which may represent a biological function in this protein. The redox potential of the $[4Fe\text{-}4S]^{2+/+}$ couple was found to be below -500 mV, which excludes an electron-transfer function for this cluster.

1. Balk, J., Pierik, A. J., Netz, D. J., Muhlenhoff, U., and Lill, R. (2004) *EMBO J.* **23**(10), 2105-2115
2. Horner, D. S., Heil, B., Happe, T., and Embly, T. M. (2002) *Trends Biochem. Sci.* **27**(3), 148-153

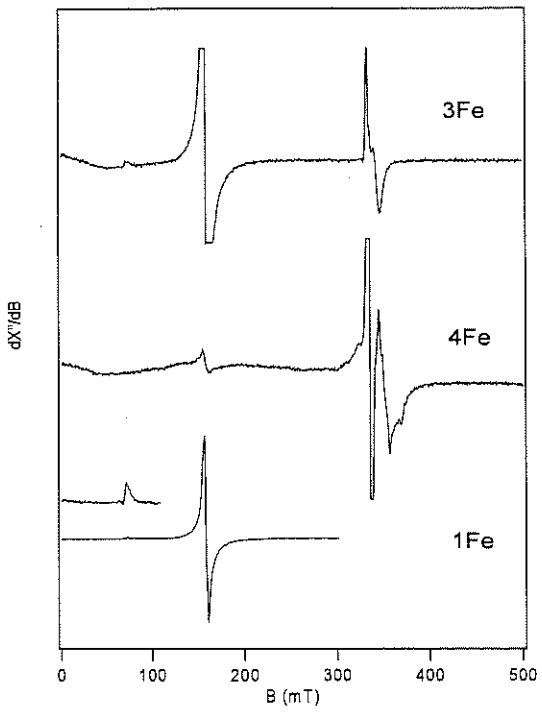

EPR spectra of *S.cerevisiae* Nar1

Inherent point defects in tensile strained (100)Si/SiO_2 entities probed by electron spin resonance.

P. Somers, V. V. Afanas'ev, and A. Stesmans

Department of Physics, University of Leuven, Celestijnenlaan 200D, 3001 Leuven, Belgium

The application of biaxial tensile strained-Si (sSi) layers is known to result in a substantial improvement (up to >100%) of the carrier mobility (μ) in inverted channels of Si-based complementary metal-oxide-semiconductor (CMOS) structures. As presently understood this strain will improve the electron mobility through the reduction of intervalley scattering and carrier effective mass as a result of lifting of the six-fold degeneracy of the Si conduction band minima. However, in a recent work, it was pointed out that, at least in some cases, this model could not fit the experimental data. The origin of the lack in understanding was tentatively traced down to an interface related effect. Not only an increase in mobility but also improved low frequency noise characteristics were observed in sSi based devices compared to standard Si. This decrease in 1/f noise was attributed to a lower density of defects in the SiO_2 near the (100)Si/SiO_2 interface. These results suggest a change in the (near)-interfacial properties of the sSi/SiO_2 structure compared to standard unstrained Si/SiO_2. The current work uses ESR active inherently occurring defects located at and near the interface as probes to compare the interface and oxide quality of (100)sSi/SiO_2 and standard (100)Si/SiO_2 structures.

Comparative electron spin resonance studies are reported on (100)Si/SiO_2 entities, grown by thermal oxidation at 790°C (1.1 atm O_2) of sSi layers, epitaxially grown on a strain relaxed $Si_{0.8}Ge_{0.2}$ buffer, and standard (100)Si. In the as-oxidized state a significant decrease (50%) of inherently incorporated interface defects, P_{b0} and P_{b1}, is observed, i.e., the sSi/SiO_2 interface is found to be inherently significantly improved in terms of electrically detrimental interface traps P_{b0}. After VUV irradiation two more defects appear, namely $E'_{\square}$ ($O_3{\equiv}Si^{\bullet}$ entity at the site of an O vacancy) and EX. Interestingly a decrease in $E'_{\square}$ defect density (~50%) is observed compared to standard Si/SiO_2, i.e., the SiO_2 thermally grown on sSi is of improved quality in terms of oxygen vacancies. This reduction in inherent electrically active interface (P_{b0}) and near-interface ($E'_{\square}$) traps would establish sSi/SiO_2 as a superior device structure for all electrical properties where (near-)interfacial traps play a detrimental role. For one, the reduction of detrimental (near-)interface defects may be an additional reason for the commonly reported mobility enhancement in sSi/SiO_2 based MOS structures over standard Si/SiO_2 ones, and at the same time account for the reported reduction of 1/f noise in the former structures. The data also confirms the generally accepted notion that P_b-type defects are mismatch induced defects.

HIGH RESOLUTION 2D AND 3D EPR MOLECULAR IMAGING OF MELANIN IN MELANOMAS

E.S. Vanea, N. Charlier, M. Dinguizli, J. Dewever, O. Feron, and B. Gallez
Laboratory of Biomedical Magnetic Resonance, Avenue Mounier 73, Université Catholique de Louvain, B-1200 Brussels, Belgium

Introduction and Objectives of the study

The incidence of malignant melanoma is increasing at alarming rates. Prevention, early detection, appropriate clinical and histological diagnoses are critical to favourable outcomes. If a lesion is suspicious for melanoma, adequate biopsy is necessary for staging and management. Thicker melanomas (Breslow thickness greater than 1mm) show greater risk of metastatic disease. In case of suspicious melanoma, there is a need to conduct a sentinel lymph node biopsy technique. Finally, the early detection of metastasis (in liver or lungs) may improve the long-term survival of patients. Our work is dealing with the development of new methods allowing the selective high resolution imaging of melanomas. Melanin are amorphous, irregular, polymeric pigments that contain organic free radicals of o-semiquinone type. We hypothesized that the most recent developments in EPR imaging could make this technique a suitable method to map these free radicals with high sensitivity and high resolution, and render 3D-imaging of these malignant tissues.

Methods and Materials

Melanoma B16 were implanted in C57Bl6 mice. Melanomas and metastatic lungs were sampled and freeze-dried. A variety of spatial and spectral-spatial (2D and 3D) EPR images have been performed on whole intact melanoma samples and metastatic lungs using a X band system (ELEXSYS E 540). *In vivo* EPR techniques, 1.1 GHz, using advanced surface and/or whole body coils were used to provide a signal from melanin and to image a melanoma.

Results

Melanin complexes in melanomas present at room temperature an EPR signal with a g value of 2.005, and a line width of ca 7 G. Using appropriate gradients (49 G/cm), it was possible to obtain 2D and 3D images (Fig 1 and 2) with a high resolution (250µm/pixel). 2D and 3D EPR imaging give us unprecedented quantitative and qualitative information concerning the spatial distribution of paramagnetic melanin radicals in these tumors. For the first time we were able to detect and image in vivo these endogenous radicals in SC melanoma implanted in mice (Fig 4 and 5).

Conclusions and Perspectives

EPR imaging can provide unique information concerning the spatial distribution of the free radicals (in special melanin complexes) in melanoma and melanoma metastases.

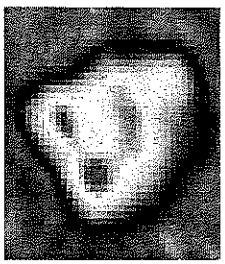

Fig. 1 2D EPR Image of B16-Melanoma

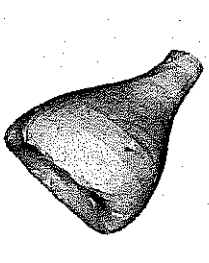

Fig. 2 3D EPR Image of B-16 Melanoma

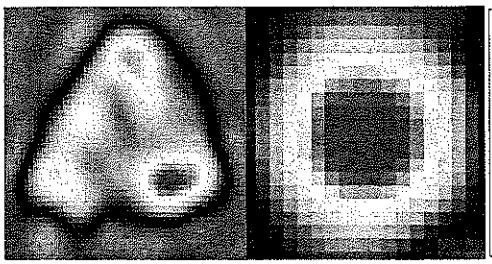

Fig. 3 2D EPRI of a metastasic lung

Fig. 4 2D EPRI of melanoma ***in vivo***

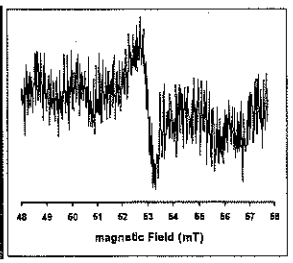

Fig. 5 ***In vivo*** EPR spectrum of melanoma

The distance between a native cofactor and a spin label by a two-frequency pulsed electron paramagnetic resonance method (DEER)

Igor V. Borovykh[1,2] , Stefano Ceola[3], Prasad Gajula[1] , Sergey Milikisyants[3], Peter Gast[2], Heinz-Jürgen Steinhoff[1], Martina Huber[3]

[1]*Fachbereich Physik, Universität Osnabrück, P. O. Box , 49069 Osnabrück, Germany;*
[2]*Department of Biophysics, Huygens Laboratory, Leiden University, the Netherlands.*
[3]*Department of Molecular Physics, Huygens Laboratory, Leiden University, P.O. Box 9504, 2300 RA Leiden, the Netherlands.*

Methods for distance determination in biological systems are sought to obtain structure information in cases where the more conventional methods, such as X-ray crystallography, cannot be applied. This is often the case for membrane proteins, in particular when investigating conformational changes related to electron-transfer events. Given the large influence of the donor-acceptor distance on the electron-transfer rates, and the importance of conformational changes in the regulation of these processes, structural information is of particular relevance.
Here, the distance between the paramagnetic state of a native cofactor and a spin label is measured in the photosynthetic reaction centre of *Rhodobacter sphaeroides* (R26), using a two-frequency, pulsed electron paramagnetic resonance method (double electron electron spin resonance – DEER). A distance of 3.05 nm between the semiquinone-anion state of the primary acceptor (Q_A) and the spin label at the native cysteine at position 156 in the H-subunit is found. Molecular-dynamics (MD) simulations are performed to interpret the distance. A 6 ns run comprising the entire RC protein yields a distance distribution that is close to the experimental one. The average distance found by the MD simulation is smaller than the distance obtained by DEER by at least 0.2 nm. Several possible reasons for this difference are discussed.

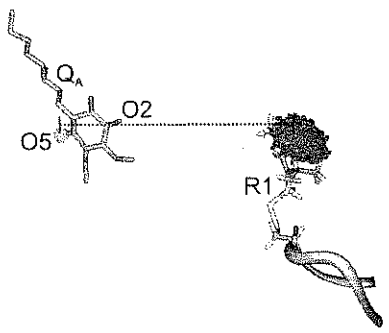

EPR and ENDOR investigation of the positive polaron in the doped polymers MDMO-PPV and P3HT

A. Aguirre[1,*], G. Janssen[1], E. Goovaerts[1], S. Van Doorslaer[1], S. Orlinski [2], E. Groenen[2]

[1] *Department of Physics - CDE, University of Antwerp, Universiteitsplein 1, B-2610 Antwerpen, Belgium.*
[2] *Leiden University, Huygens Laboratory, MoNOS, NL-2300 RA Leiden, The Netherlands*

Organic solar cells are promising as an efficient, environmentally friendly and low cost energy production technology. In the 3D heterojunction solar cell device based on blends of conjugated polymers and fullerene derivatives, the polarons in the polymer component play a key role as positive charge carriers. While in the PV process the polarons result from charge transfer to a fullerene acceptor, they can also be induced by chemical reduction using a doping agent such as molecular iodine. We report a detailed EPR and ENDOR investigation of these radical states in doped P3HT and MDMO-PPV, the standard polymers presently in use in state-of-the-art devices.

Spin coating of these polymers is shown to lead to a preferential distribution of the polymer chains in the plane of the resulting films. In W-band EPR a pronounced angular dependence is observed which allows for a further assignment of the g-values to specific molecular orientations. In the case of MDMO-PPV, the principal direction with largest g-value lies along the polymer backbone, while in P3HT, this direction carries the smallest g-value. The degree of preferential orientation is evaluated by comparison with spectral simulations.

X-band HYSCORE as well as Q-and W-band ENDOR experiments have revealed a distribution of proton hyperfine interactions, in agreement with a description of a polaron extending over a number of polymer units. Based on the spin distribution of the polaron over the polymer chain, available for both polymers from *ab-initio* calculations [1], consistent simulations of the HYSCORE and ENDOR spectra could be achieved using the well known McConnell relation [2] for a hydrogen bound to carbon in a conjugated chain. For MDMO-PPV, the effect of slow relaxation on the Q-band ENDOR spectrum directly demonstrates the negative sign of the proton hf parameters.[#] Finally, ^{13}C interactions could be detected in HYSCORE as well as ENDOR spectra in both polymers, and will be discussed in terms of the spin densities on neighboring atoms.

[1] Brendel P., Grupp A., Mehring M. Synth. Metals 45 (1991) 49-57; Geskin V. M., Dkhissi A., Bredas J. L., Int. J. Quant. Chem., 91 (2003) 350.
[2] McConnell H.M., Chesnut B., Journal of chemical Physics 28(1958)107-117.

* Corresponding author: Aranzazu.Aguirre@ua.ac.be

Q-band ENDOR measurements performed at the Millimeter Wave and High-Field ESR Laboratory, St Andrews, Scotland, are kindly acknowledged.

Enhanced release of nitric oxide from endothelial cells under anoxia.

Ernst van Faassen,

Faculty of Science, Interface Physics,
Ornstein Laboratory, Utrecht University.
3508 TA, Utrecht, The Netherlands.

The mammalian enzyme Endothelial nitric oxide synthase (eNOS) synthesizes NO radicals from arginine in a tightly regulated enzymatic cycle that consumes oxygen. This cycle is a central process in the regulation of blood pressure in mammals and man. In absence of oxygen, this normal pathway for NO is blocked and vascular flow is reduced by constriction of blood vessels. However, we found that eNOS may release NO from nitrite anions as an alternative pathway under anoxia. The anoxic release of free NO was verified by three independent methods: Electrochemically with an NO-sensitive electrode, by EPR spin trapping with iron-dithiocarbamate complexes and by optical absorption spectroscopy. EPR spin trapping with ^{15}N-labelled nitrite proved unambiguously that the NO was generated from nitrite anions.

We propose that the anoxic nitrite reductase pathway might provide a significant alternative source of NO for tissues under acute hypoxia. This hypothesis was tested in cultured endothelial (bEND.3) cells. Anoxia was imposed by flushing with argon. Anoxia significantly enhanced (!) the release of NO from the cells over normoxic conditions. NO was detected EPR spin trapping during 20 minutes at 37° C. The basal NO yield from 7.5 x 10^6 confluent cells was 110 pmole. Under anoxia, this yield was increased to 160 pmole. The anoxic NO release could be cancelled by specific NOS inhibitors NLA and L-NAME. The anoxic NO release was sustained for 30 minutes and accompanied by a decrease in the intracellular nitrite concentration.

Yields of NO-trapping adducts (in pmol) in 7.5±0.5 x 10^6 endothelial cells. Trapping proceeded for 20 min at 37° C. The second row gives the preincubation times τ_{inc} of the supplements. During preincubation the cells were kept at 37° C in an atmosphere with 5% CO_2 and 20% O_2.

	Basal unstimulated	Stimulated with CaI (5 µM)	NLA (57 µM)	L-NAME (5 µM)	L-NAME (50 µM)	Imidazole (10 mM)	Oxypurinol (100 µM)	$NaNO_2$ (250 µM)
τ_{inc}	--	--	20'	2'	2'	1'	20'	20'
oxia	110±8	400± 30	†	93± 10	51± 8	85± 10	n.d.	116±8
anoxia	160± 10	n.d.	†	87± 8 ¶	61±8	80±10	170± 10	154±8

† below detection limit of ca 10 pmole.
¶ 85 ± 8 pmole with τ_{inc} = 20'

Conclusion: Imposition of anoxia causes a strong release of NO from cultured endothelial cells under consumption of intracellular nitrite. The magnitude and duration of the nitrite reduction suggests that the phenomenon have physiological relevance for NO levels near the endothelium under acute hypoxia where the normal enzymatic activity is blocked by the absence of oxygen.

ABSTRACTS

Posters

Local field properties of $PbWO_4$ scintillating crystals doped with transition ions

M. Stefan[1], S. V. Nistor[1], E. Goovaerts[2], F. F. Popescu[3], V. Bercu[3,4], M. Martinelli[4] C.A.Massa[4], L.A.Pardi[4] and M. Nikl[5]

[1]*National Institute for Materials Physics, Bucharest, Romania*
[2]*Department of Physics - Campus Drie Eiken, University of Antwerp, Belgium*
[3]*Department of Physics, University of Bucharest, Romania*
[4]*Institute for Chemical and Physical Processes, CNR, Pisa, Italy*
[5]*Institute of Physics AS CR, Prague, Czech Republic*

Lead tungstate – $PbWO_4$ (PWO) is presently one of the most studied materials in the scintillator oriented research, due to its approved applications in the detectors of high-energy physics accelerators and for other domains as medical imaging, radiation defectoscopy, safety sector, etc. A significant result in the optimization of PWO for the above applications was achieved by the selected trivalent ion doping at the Pb^{2+} site, which efficiently compensated/suppressed the intrinsic trapping states in the forbidden gap of PWO.

Information about the defects properties is paramount for an educated choice of dopants in order to design and control specific material properties. Electron Paramagnetic Resonance is one of the best suited techniques to provide such essential information about the local interactions, microstructure and quantum properties of defects.

We report here the results of extensive comparative multifrequency EPR studies on PWO single crystals doped with rare earth ions of different valencies (Mn^{2+}, Gd^{3+}, Nd^{3+}, etc.). The main focus of these studies is the evaluation of the local crystal field properties and energy transfer mechanisms.

Point defects in phase-separated SiO/SiO_2 superstructures analyzed by electron spin resonance

M. Jivanescu[1], A. Stesmans[1], S. Godefroo[2] and M. Zacharias[3]

[1]*Department of Physics, University of Leuven, Celestijnenlaan 200 D, B-3001 Leuven, Belgium*
[2]*INPAC-Institute for Nanoscale Physics and Chemistry, University of Leuven, Belgium*
[3]*Institute of Microstructure Physics, Weinberg 2, 06120 Halle, Germany*

With the integrated circuit device technology being majorly built on silicon as basic semiconductor, it is quite natural that the study of optical activity (light emission) of Si has attracted much attention. In this respect, one variant of Si that has been intensively studied is porous silicon, with promising results [1]. Yet, main problems here imply its fragility and high surface reactivity. So, other directions have been investigated. A different type of nanostructure studied consists of Si nanoparticles embedded in an oxide matrix, SiO_2 in the case of the samples investigated here. Such structures were observed to exhibit an interesting photoluminescence, which has evoked much interest for potential applications [2]. The current work reports on high-sensitivity ESR analysis on nano-Si particles/SiO_2 superstructures fabricated by the SiO/SiO_2 superlattice approach with the intent, in a first approach, to reveal, categorize, and quantify occurring paramagnetic defects, both in the as prepared sample and after applying different types of irradiation. Based on the knowledge of the atomic nature of the revealed ESR active defects, we asses the location of these centers, i.e., with what specific feature of the structure the separate types of defects are related to, as well as the potential (detrimental) influence of these centers on the photoluminescence properties.

It appears that the phase-separated SiO/SiO_2 superstructures exhibit a substantial density of inherent point defects (P_b type defects, D, EX, and E' centers), related either with the embedded Si particles or the SiO_2 matrix. We found that some type(s) of those paramagnetic defects do affect the photoluminescence substantially, and should thus be tightly controlled. The provisional conclusion is that both defects and quantum confinement play a decisive role in the photoluminescence of phase-separated SiO/SiO_2 superstructures.

[1] Z. Yamani, A. Alaql, J. Therrien, O. Nayfeh, M. Nayfeh, Appl. Phys. Lett. **74**, 3483 (1999).
[2] M. Zacharias, J. Heitmann, R. Scholz, U. Kahler, M. Schmidt, J. Blasing, Appl. Phys. Lett. **80**, 661 (2002).

High frequency (95Ghz) ESR investigations of paramagnetic point defects in superhard cubic boron nitride single crystals

S. V. Nistor[1], M. Stefan[1], E. Goovaerts[2] and T. Taniguchi[3]

[1] *National Institute for Materials Physics, P.O. B MG-7 Magurele-Bucuresti, 077125 Romania*
[2] *Department of Physics-CDE, University of Antwerp, Universiteitsplein 1, Antwerpen(Wilrijk), 2610 Belgium*
[3] *National Institute for Materials Science, 1-1 Namiki, Tsukuba, 305-0044, Japan.*

The cubic phase of boron nitride (c-BN) with cubic sphalerite structure is the most amazing semiconductor, surpassing even the diamond by its largest known band gap of 6.25 eV, the possibility to be both *p*- and *n*-type doped as well as its extremely high thermo-chemical stability. Because c-BN is usually available in sub millimeter sized crystals the best way to investigate the properties of the defects/impurities involved in the semiconducting properties is by high frequency (W-band) ESR measurements on such oriented single crystallites. Using this approach we have already identified several types of paramagnetic centers in dark c-BN crystals prepared with boron excess [2], in a Be-doped blue c-BN crystal [2] and in amber colored c-BN crystals [3].

We shall present the results of a (95GHz)-band ESR investigation on several types of c-BN single crystals of various colors, obtained by high temperature – high pressure synthesis with different starting compositions and impurities. The measurements have been performed at temperatures as low as 10K before, during and/or after "in situ" illumination with an Ar^+-laser, at 488nm wavelength. It was found out that the content of paramagnetic defects strongly depends on the conditions of crystal growth, reflected also in their coloration. It was also found out that the samples which did not exhibit ESR spectra in the as-grown state do exhibit such spectra by "in-situ" irradiation. The results will be discussed in connection with previous published studies concerning the presence and properties of impurities in the c-BN crystal lattice.

References:

[1] S. V. Nistor, M. Stefan, D. Schoemaker, E. Goovaerts and G. Dinca, *Diam. & Rel. Mater.* **10**, 1408 (2001).
[2] E. Goovaerts, S. V. Nistor, D. Ghica and T. Taniguchi, *Phys. Stat. Sol.* **a201**, 2591 (2004)
[3] S. V. Nistor, D. Ghica, M. Stefan, A. Bowen and E. Goovaerts (to be published)

A multi-frequency EPR study of $Co(II)S_4$ coordination

S. Milikisyants[1], D. Maganas[1], H. Blok[1], P. Gast[1], A. Grigoropoulos[2], P. Kyritsis[2], G. Pneumatikakis[2], J.M.A. Rijnbeek[1], S. Sottini[1] and E.J.J. Groenen[1]

[1] *Department of Molecular Physics, Leiden University, The Netherlands*
[2] *Department of Chemistry, University of Athens, Greece*

Extensive crystallographic studies during the last few years have revealed the existence of M-S bonds in the active site of many metalloenzymes, most prominently with the transition metals M=Fe, Ni, Cu, Zn, Mo, W. Besides these metals, one should also consider Co, since it has recently been shown that the enzyme ATP sulfurylase is a metalloenzyme containing Co(II) and Zn(II) in its active site. Moreover, to enable spectroscopic and magnetic investigations, Zn(II)- or Cd(II)-containing active sites of enzymes are frequently reconstituted with Co(II). The relevance of cobalt-sulfur coordination for biological systems has prompted us to synthesize and investigate by EPR and ENDOR model complexes of cobalt with sulfur-containing bidentate ligands LH of the type $R_2PSNHPSR_2'$ where R, R' = phenyl, isopropyl.

The large zero-field splitting of divalent cobalt $\left(S=\frac{3}{2}\right)$ calls for a multi-frequency approach.
We report cw and pulsed EPR experiments at X-, W-, and J-band, from room temperature down to liquid-helium temperatures. We have investigated solutions, powders and crystals of complexes in (pseudo-)tetrahedral geometry. In order to decrease the linewidth (increase the resolution), use has been made of diluted samples in which cobalt is largely replaced by zinc, which is EPR silent. Based on the zero-field splitting and the anisotropy of both the g matrix and the cobalt hyperfine interaction, we will discuss the electronic structure of the cobalt coordination. In addition, we will indicate the possibilities of future ENDOR experiments, which aim at the quantitative analysis of the covalent character of the cobalt-ligand interaction.

Factors determining the enantio-selectvity of *R*-, and *S*-methylbenzylamine by chiral copper(II) salen-type complexes

I.Caretti[1], D.M. Murphy[2], I.A. Fallis[2], M. Goebel[2], D.J. Willock[2], J. Landon[2] and S. Van Doorslaer[1].

[1]*University of Antwerp, Department of Physics, SIBAC laboratory, Universiteitsplein 1, B-2610 Wilrijk, Belgium.*
[2]*School of Chemistry, Cardiff University, Main Building, Park Place, Cardiff CF10, 3AT, UK.*

Chiral complexes formed by incorporation of transition metal ions into the tetradentate Schiff Base ligand derived from salicylaldehyde and ehtylenediamine (metal salenes), have been widely studied in the framework of asymmetric catalysis. The main advantages of salen derivates over the well-known pophyrins reside in the higher simplicity of the preparation method and the localization of the stereogenic centres close to the metal center, facilitating the induction of an asymmetric environment around it.[1,2]
Driven by the demand of optically pure compounds, the metal complexes of the Schiff base *N,N'*-bis(3,5-di-tert-butylsalicylidene)-1,2-cyclohexane-diamine introduced by Jacobsen *et al* [3] have been successfully tested as catalysts in many enantioselective reactions. [4] Specifically, symmetric substitution of tert-butyl groups in the phenol part of the salen ligand generates compounds with a good enantiomeric excess in the epoxidation of unfunctionalized alkenes, epoxide ring opening, hydrolytic kinetic resolution of racemic epoxides, cyclopropanation. However, further research needs to be done to completely unravel how the catalytic process works and what interactions are determinant in the asymmetric catalytic process.
In this work we investigate the ability of two chiral copper(II) Jacobsen complexes Cu**[1]** and Cu**[2]** (Figure 1) to discriminate between the *R*- and *S*- forms of methylbenzylamine (MBA). This enantio-selectivity can be detected by subtle differences in the continuous wave (CW) EPR&ENDOR spectra of the (*SS-S, RR-R*) and (*SS-R, RR-S*) Cu**[1,2]**/MBA pairs.. Both the X-Band CW EPR&ENDOR and W-Band CW EPR, as well as the ELDOR-detected NMR spectra, of the above cited homochiral sets show a preferential formation of the *SS-R* and *RR-S* adducts compare to the alternative pair-wise combinations. This phenomenon seems to be connected to the degree of symmetry of the copper centre for both copper compounds. Our results are consistent with DFT calculations, which also reveal the importance of the π-π stacking and the bulkiness of the MBA molecule in assisting the enantio-selectivity process.

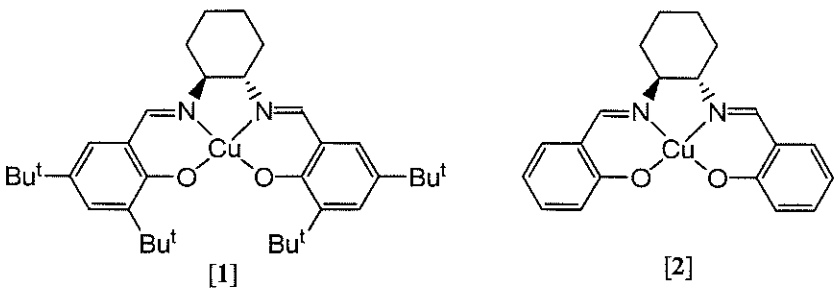

[1] [2]

Figure 1

References:

[1] Tehshik P.Yoon and Eric N. Jacobsen, *Science* 2003, **299**,1691.
[2] Q.-H. Xia, H.-Q. Ge, C.-P. Ye, Z.-M. Liu and K.-X. Su, *Chem. Rev.* 2005, **105**, 1603.
[3]Tokunaga; M.; Larrow, J.F.; Kakiuchi, F.; Jacobsen, E.N., *Science*, 277, 936 (1997)
[4] Laetitia Canali and David C. Sherrington, *Chem. Soc. Rev.*, 1999, **28**, 85.

The heme-pocket structure of globin-like molecules from *C. Elegans*

Evi Vinck[1], Sabine Van Doorslaer[1], Nóra Nagy[1], Liesbet Thijs[2], Sylvia Dewilde[2], Luc Moens[2]

[1] *Department of physics, University of Antwerp, Belgium*
[2] *Department of biomedical sciences, University of Antwerp, Belgium*

Recently, 33 globin-like sequences have been identified in the genome of the nematode worm *C. elegans* [1], all of which are expressed. The corresponding proteins have unknown functions. In this work, the geometric and electronic structure of the heme-pocket region of two globin-like *C. elegans* molecules is determined with EPR techniques. Both globins show a significantly different structure: The "ZK637.13" globin is predominantly found in a high-spin state, whereas the "T22C1.2" globin is characterized by a low-spin bishistidine coordinated form, with nearly perpendicular aligned axial imidazole planes. The structural characteristics are compared in detail with known mammalian myoglobins, hemoglobins, and neuroglobin.

References

[1] Hoogewijs, D., Geuens, E., Dewilde, S., Moens, L., Vierstraete, A., Vinogradov, S., & Vanfleteren, J., *IUBMB.Life* 56, 697-702 (2004);
Vinogradov, S., Hoogewijs, D., Bailly, X., Arredondo-Peter, R., Gough, J., Dewilde, S., Moens, L., & Vanfleteren, J. A, *BMC.Evol.Biol.* 6, 31 (2006);
Vinogradov, S. N., Hoogewijs, D., Bailly, X., Arredondo-Peter, R., Guertin, M., Gough, J., Dewilde, S., Moens, L., & Vanfleteren, J. R., *Proc.Natl.Acad.Sci.U.S.A* 102, 11385-11389 (2005)

An inside view on high-spin and low-spin ferric heme proteins- Application on neuroglobin

F. Trandafir[1], M. Fittipaldi[1,2], J. Harmer[3], S. Dewilde[4], L. Moens[4], S. van Doorslaer[1]

[1]*Department of Physics, University of Antwerp, B-2610 Wilrijk- Antwerp, Belgium*
[2]*Department of Chemistry, University of Florence, I-50019 Sesto Fiorentino, Italy*
[3]*Laboratory of Physical Chemistry, ETH Zurich, 8093 Zurich, Switzerland*
[4]*Department of Biomedical Science, University of Antwerp, B-2610 Wilrijk-Antwerp,Belgium*

One of the members of the globin family, neuroglobin, is still creating debates on the structural and functional aspects even if, it was discovered almost 7 years ago. In this challenging environment we try to have a close look at the heme pocket of human neuroglobin (NGB) and of its E7-Gln mutant using the advantages offered by multi-frequency pulsed EPR techniques. To better understand the structure-function relation of the protein also the cyanide adducts of the two proteins are analysed.
Different X-band HYSCORE schemes in combination with W-band ELDOR-detected NMR are used to study the hyperfine and nuclear-quadrupole couplings of the heme and the histidine nitrogens of ferric E7-Gln NGB (a high-spin system) in comparison to aquometmyoglobin. The simulation and interpretation of HYSCORE spectra of these types of S=5/2, I=1 systems will be elucidated. Comparative HYSCORE experiments combined with deuterium exchange experiments for aquometmyoglobin and ferric E7Q-NGB clearly show that the heme iron of the latter protein is pentacoordinated, lacking the distal water.
Due to the complexity of the X-band HYSCORE spectra, the peak assignment for different signals stemming from the nitrogen atom of the cyanide and the ones coming from histidine and porphyrin ring is difficult. As a possible solution for this problem, measurements are performed on isotope labelled ($^{13}C^{14}N$ and $^{12}C^{15}N$) cyanide adducts. Pulsed ENDOR techniques have to be used in combination with ESEEM in order to obtain the full characterisation of these systems.

PROBING THE HEME-POCKET STRUCTURE OF THE PARAMAGNETIC FORMS OF CYTOGLOBIN AND ITS E7Q MUTANT USING ELECTRON PARAMAGNETIC RESONANCE

A. I. Ioanitescu[1], S. van Doorslaer[1], S. Dewilde[2], B. Endeward[3], L. Moens[2]

[1]*Department of Physic, University of Antwerp, Antwerp, Belgium,*
[2]*Department of Biomedical Sciences, University of Antwerp, Antwerp, Belgium,*
[3]*Institute for Physical and Theoretical Chemistry, JW Goethe University, Frankfurt am Main, Germany*

Cytoglobin is a recently discovered vertebrate globin. EPR spectroscopy was used to investigate different paramagnetic forms of wild-type human cytoglobin (CYGB) and its E7Q mutant. In addition, the □Cys mutant of CYGB (Cys→Ser) was analysed and compared with the wild-type (wt) form. The ferric form of CYGB showed predominantly a bis-histidine legation (F8His-Fe^{3+}-E7His), which differs from the known forms of mammalian hemoglobins and myoglobins. The heme-pocket structure of ferric wt CYGB using S- and X-band pulsed EPR methods was determined. The data also allow the solution of an earlier conflict between two x-ray diffraction studies [1,2]. In the second part, X-band EPR techniques are applied to study the heme-pocket environment of ferric E7Q-CYGB. No distal water is coordinating to the heme iron in this mutant. The hyperfine and nuclear quadrupole couplings of the directly coordinating heme and hisitinde nitrogens in ferric wt CYGB and E7Q-CYGB are derived and compared with known data on other ferric porphyrin compounds. In a final part, X-band CW EPR techniques are used to establish that NO can bind to cytoglobin in *E. coli* cells over-expressing this globin. All results are in detail compared to the findings of similar studies performed on neuroglobin, another newly discovered member of the vertebrate globin family that is known to exhibit bis-histidine coordination of the heme iron in both the ferrous and ferric form of the protein.

[1] De Sanctis D., Dewilde S., Pesce A., Moens L., Ascenzi P., Hankeln T., Burmester T., and Bolognesi M. (2004) *J. Mol. Biol.* **336**, 917-927
[2] Sugimoto H., Makino M., Sawai H., Kawada N., Yoshizato K., Shiro Y. (2004) *J. Mol. Biol.* **339**, 873-885

The globin-coupled sensor of *Geobacter sulfurreducens*, characterisation by means of EPR and resonance Raman spectroscopy

F. Desmet[1], L. Thijs[2], S. Dewilde[2], L. Moens[2] and S. van Doorslaer[1]

[1]*Department of Physics, University of Antwerp, Universiteitsplein 1, B-2610 Wilrijk, Belgium*
[2]*Department of Biomedical Sciences, University of Antwerp, Universiteitsplein 1, B-2610 Wilrijk, Belgium*

The capability to sense fluctuating levels of oxygen is of key importance for the adaptation of living organisms to a variable environment. Globin-coupled sensors (GCS) are multi-domain hemoproteins that combine a globin domain with a second transduction domain. Binding of molecular oxygen and other diatomic gaseous ligands, such as carbon monoxide and nitric oxide, to the heme of the globin domain triggers the signal transduction domain. However, at present, little is known about the nature of this mechanism.
We present here the results of continuous-wave and two-dimensional pulsed EPR experiments together with optical resonance Raman spectra of the globin part of the GCS of *Geobacter sulfurreducens*. The data will be translated into structural information of the heme pocket. This analysis is the first step in a detailed study of the structure-function relationship of this globin-coupled sensor.

Structure determination of neuroglobin using EPR

M. A. Ezhevskaya[1], E. Vinck[1], S. Dewilde[2], L. Moens[2], S. van Doorslaer[1]

[1]*Department of Physics, University of Antwerp, Universiteitsplein 1, B-2610 Wilrijk, Belgium*
[2]*University of Antwerp, Department of Biomedical Sciences, Universiteitsplein 1, B-2610 Wilrijk, Belgium*

7 years after the discovery of vertebrate neuroglobins, their function and structure-function relationship is still not known. Spectroscopic techniques evidently play an important role in the strategies that are being developed to shed light on this surprising globin. In this contribution, we show how EPR can be used to extract structural information about neuroglobin.

We want to show how structural aspects of the full Ngb protein can be studied by introduction of a nitrosyl spin-label in the protein. For that purpose two kinds of spin labels are used: 4-(2-Iodoacetamido)-TEMPO and (1-Oxyl-2,2,5,5,-tetramethylpyrrolidin-3-yl) methyl methanethiosulfonate (MTS). The heme iron can be either in a paramagnetic state (ferric form, NO-ligated ferrous form, ...) or in a diamagnetic form (low-spin ferrous form, oxy ferrous form, ...). By attaching a spin label at a specific site in the neuroglobin protein chain using site-directed mutagenesis and varying the characteristics of the heme iron site, we can in principle reveal information about the Fe-spin label distances and protein dynamics using EPR. The basis of this procedure will be outlined. The present study is focussed to reveal information on the CD corner of the neuroglobin protein, a region where the X-ray data show low resolution. For this the GCS, CSS and SSC mutants of human neuroglobin are labelled with the different spin labels. The problems related to changing the spin state of the heme side in the presence of the spin-label will be highlighted and the first EPR results will be shown.
It will also be shown that the present strategy can serve as a model study for elucidating structural aspects of globin-coupled sensors.

Imidazole as an anchor donor group in oligopeptide – copper(II) equilibrium systems

Nóra Veronika Nagy[1], Tamás Gajda[2], Bernard Henry[3] , Patrick Gizzi[3], Zoltán Paksi[2], Antal Rockenbauer[1]

[1]*Chemical Research Center of the Hungarian Academy of Sciences, P.O. Box 17 H-1025 Budapest , Hungary*
[2]*Department of Inorganic and Analytical Chemistry, University of Szeged, Hungary*
[3]*Université Henri Poincaré Nancy, France*

In an aqueous solution of small peptides and metal ions a number of complexes of different compositions, stabilities and structures are generally formed by stepwise deprotonation of the amid-NH groups. This deprotonation can be promoted by the coordination of a stronger anchor (terminal) donor group. In order to clarify the function of the Imidazole-N and amino-NH_2 as anchor donor groups we aimed to compare the equilibrium systems of copper(II) - triglycylhistamine (GGGHa) and – t-butyloxycarbonyl-triglycylhistamine (BGGGHa) using EPR methods.

A series of X-band CW EPR spectra were recorded at room temperature in different pH's and ligand to metal concentration ratios for both systems. The titration was performed in a circulating system in order to ensure the same instrumental conditions during the measurements. All the registered spectra were simulated simultaneously with the 2D_EPR program[1] developed for the decomposition of overlapping isotropic EPR spectra of paramagnetic metal complexes. The program can provide the isotropic EPR parameters as well as the formation constants of the species.

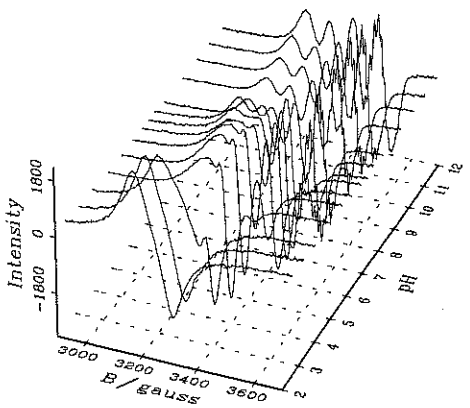

In the BGGGHa – copper(II) system we could follow the stepwise deprotonation starting from the imidazole-N, as the amino-NH_2 group was protected. In ligand excess *bis*-complexes were also identified with the ligation of a second ligand via its imidazole-N. Having two strong terminal donor groups the complexation properties changed notably for GGGHa. For most of the complexes both terminal nitrogens found to be coordinated to the same copper(II)ion, but with linking of two different copper(II)ions formation of oligomers was also detected. From comparison with the data from the BGGGHa system, it was established that the anchor donor group for the GGGHa ligand is also an imidazole-N.

[1]Rockenbauer, A.; Szabó-Plánka, T.; Árkosi Zs.; Korecz, L.; *J. Am. Chem. Soc.* **2001**. 123, 7646-7654

Electron spin resonance characterization of P-related point defects in nm-thick HfO_2 layers of (100)Si/HfO_2 entities and ZrO_2 insulators.

K. Clémer, A. Stesmans, and V. V. Afanas'ev

Department of Physics, University of Leuven, 3001 Leuven, Belgium

The relentless scaling of Si/SiO_2-based complementary metal-oxide-semiconductor (CMOS) transistors will require the replacement of the conventional SiO_2 gate dielectric. One of the leading high-κ contenders are Hf-based insulators, with a main focus on nitrided Hf-silicate [1]. However, this planned replacement of the gate dielectric still faces various obstacles. One item pertinent to device processing concerns the indication of enhanced P penetration through HfO_2 or Hf silicate layers compared to SiO_2 [2], which may have a detrimental influence on device performance. A concern deals with the electronic behavior of the Si dopant atoms when penetrating into the insulator, e.g., potentially operating as charge traps and/or recombination centers. Crucial here, of course, will be how the pertinent electronic energy levels of the impurity defect sites will be positioned relative to the Si band structure (band gap). Obviously, further insight here may benefit significantly from detailed atomic understanding of the defect sites.

Results are presented of the first observation by electron spin resonance of P-related point defects in nm-thick HfO_2 films on (100)Si after annealing in the range 500-900 °C and in ZrO_2 powder –two oxides prominent in current high-κ insulator research. Based on the principal g matrices and hyperfine tensors inferred from consistent X, K, and Q-band spectra simulations and comparison with established P-associated defects in silica [3], both centers appear similar in nature and are assigned to a P_2-type defect –a P substituting a Hf or Zr atom. Both centers were observed in the monoclinic phase of the high-κ oxides with the unpaired electron strongly localized on the P atom. A steric model of the adduced P_2-type defect observed is depicted in Fig. 1. Measurement of defect densities indicates that a sizeable fraction of the phosphorus atoms present in the dielectric matrix results in a P_2 defect. It is of importance to obtain a good understanding of the center's trapping behaviour.

[1] *International Technology Roadmap for Semiconductors*: 2005 (Semiconductor Industry Association, San Jose, CA, 2005).

[2] M. A. Quevedo-Lopez, M. R. Visoskay, J. J. Chambers, M. J. Bevan, A. Lifatou, L. Colombo, M. J. Kim, B. E. Gnade, and R. M. J. Wallace, Appl. Phys. **97**, 043508 (2005); Suzuki K., Tashiro H., Morisaki Y., and Sugita Y., Jpn. J. Appl. Phys. **44**, 8286 (2005).

[3] See, e.g., D. L. Griscom, in *Glass: Science and Technology Vol. 4B*, edited by D.R. Uhlmann and N. J. Kreidl (Academic Press, N.Y., **1990**), p. 151.

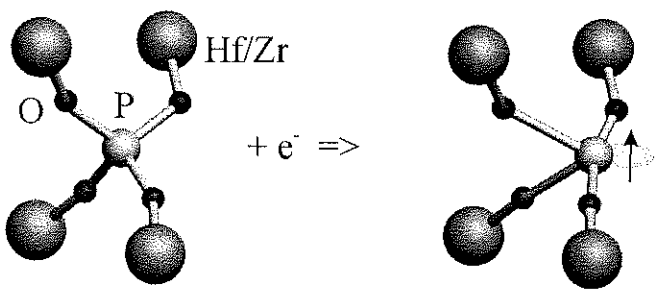

Fig. 1.

Transient and optically detected X- and W-band EPR on the triplet state of erythrosin as a model probe in biological molecules

H. Moons[1], E. Goovaerts[1], S. Van Doorslaer[1], L. Franco[2], C. Corvaja[2]

[1] *Department of Physics-CDE, University of Antwerp, Belgium*
[2] *Department of Chemical Sciences, University of Padova, Italy*

The investigation of biological molecules is often based on molecular probes –or labels- attached to them. When the probe is a stable radical purposely attached to the biomolecule the approach is called site-directed spin labeling (SDSL)[1]. It was proposed that the excited triplet state of the label, created upon illumination, may be more sensitive to specific aspects of the environment[2]. The triplet probes can be naturally occurring, e.g. tryptophan in proteins[3], or can be inserted in specific sites of the studied macromolecules, which may be called site-directed triplet labeling (SDTL). Detailed knowledge of the properties of the triplet state (g-values, zero field splitting, lifetimes, spin relaxation times,...) is required for this application.

In this project transient and pulsed EPR, as well as optically detected magnetic resonance (ODMR), –in X- and in W-band-, will be applied to investigate the triplet state of different chromophores for triplet labeling. The first probe under investigation is erythrosin (2,4,5,7-tetraiodofluorescein). In a first series of experiments we aim to obtain reference parameters for the triplet state and variations of these parameters related to the environment of the molecule. X-band ODMR spectra (phosphorescence-detected) were measured in frozen solution in propanol and in water/glycerol mixtures. Addition of the protein bovine serum albumine leads to limited but significant differences in lineshape and in the relative intensity of the half-field transition. Very different lineshapes of the triplet spectrum are obtained for X- and W-band ODMR, which is under further investigation. W-band transient EPR experiments in frozen solution and embedded in polymer film are now initiated, and the first results are being compared with parallel experiments in the X-band and literature.[4]

Corresponding author: Hans.Moons@ua.ac.be
Hans Moons, Department of Physics-CDE, University of Antwerp
Universiteitsplein 1, 2610 Antwerpen, Belgium
Hans.Moons@ua.ac.be

---

[1] W.L. Hubbell, C.A. Altenbach, *Investigation of structure and dynamics in membrane proteins using site-directed spin labelling*, Curr. Opin. Struct. Biol., 4 (1994) p. 566.
[2] M.R. Bugs and M.L. Cornélio, *Analysis of the ethidium bromide bound to DNA by photoacoustic and FTIR spectroscopy*, Photochem. Photobiol., 74(4), 512-520 (2001)
[3] A.H. Maki et al., *Spin-lattice relaxation of the tryptophan triplet state varies with its protein environment*, J. Phys. Chem. B, 106 5099-5104 (2002)
[4] D.H. Harryvan, W.H. Lubberhuizen, E. van Faassen, Y.K. Levine, G. Kothe, *Characterization of the magneto-optical properties of eosin Y and erythrosin*, Chem Phys. Lett., 257 (1996) 190.

Study of the Defect states in Thin film Silicon material by Electron spin resonance

J.K.Rath

Utrecht University, Faculty of Science, SID – Physics of Devices, P.O. Box 80,000, 3508 TA Utrecht, The Netherlands,
e-mail : J.K.Rath@phys.uu.nl

Dangling bond (db) states in a silicon material act as efficient recombination centers for photo-generated carriers and materials with low concentration of dbs are required for achieving high photosensitivity and their application in solar cells. Moreover, dbs act as good trapping states for charge carriers which determine the electric field inside an i-layer of a p-i-n type solar cell. Generally dbs in amorphous silicon material (and presumed to be so in microcrystalline silicon material) are amphoteric states and they can stay in charged or neutral states. Study of the neutral dbs, which are paramagnetic centers, has provided enormous information on the defect density, types of dbs in an alloy (Si-db and Ge-db in a-SiGe and Si-db and C-db in a-SiC etc) and their respective concentrations, kinetics of the growth of dbs with light soaking and electron irradiation, whereas LESR and ODMR have provided information on recombination process in the material.

The above experience in amorphous silicon has been extended to the microcrystalline silicon material, assuming similar density of sates and defects creation process as for the amorphous material. However, the difference lies in the distribution of defect states; (i) isolated defects (ii) paired defects. This paper describes the paramagnetic centers in a microcrystalline silicon material made by chemical vapor deposition techniques (PECVD, HWCVD). Just as in amorphous silicon a Si-db at 2.0055, attributed to isolated dbs has been identified. However, there are other types of Si-dbs (P_b center with g=2.006, coupled db-pair at g=2.005, oxygen related db at g=2.0043 and 2.0026.

Various exchange interactions between the dbs have been observed. The db line at room temperature is inhomogeneously broadened due to the randomly oriented centers. At low temperature a motional narrowing has been observed for a certain type of microcrystalline silicon material. It is attributed to the hopping of the paramagnetic centers, facilitated by diffusion of db center and exchange of the electron of a hydrogen atom between a pair of defect sites. On the other hand, for microcrystalline silicon material with a very small grain boundary region between the crystalline columns (for (220) oriented crystalline grain columns) has shown Heisenberg type exchange coupling due to overlapping of the orbitals. Pairing of spins shows anti-ferromagnetic coupling with a Weiss temperature of -136.4K.

The microcrystalline silicon material also shows an n-type of character due to the incorporation of oxygen. This is manifested by CE paramagnetic line at g=1998, attributed to the electron in the conduction band tail. This line increases in intensity with increasing illumination (LESR). A purely intrinsic material (compact microcrystalline silicon material) shows no such line even at temperatures as low as 10K.

DEVELOPMENT OF NON INVASIVE METHODS FOR THE MEASUREMENT OF TISSUE OXYGEN CONSUMPTION

C. Diepart, B.F Jordan and B. Gallez.

Laboratory of Biomedical Magnetic Resonance, Avenue Mounier 73, Université Catholique de Louvain, B-1200 Brussels, Belgium

Introduction

Oxygen is a key environmental factor in the development and growth of tumors, and their response to treatment. Tumor oxygenation depends on a balance between oxygen supply and consumption, and both should considered in developing strategies to reduce hypoxia.

The oxygen consumption rate of tumor cells can be measured by EPR using in vitro or ex vivo EPR measurement (1). The method is based on the variation of the linewidth of a paramagnetic material in the presence of consuming cells.

The aim of this work was to develop a new EPR method that should permit the non invasive study of tissue oxygen consumption.

Purpose

For that purpose, we designed protocols where pO2 is measured in tissue during a breathing challenge. During a breathing challenge with carbogen, the local pO2 is increasing. When changing gas to air, the pO2 returns to its basal value.

Our hypothesis is that the return kinetics is essentially due to local oxygen consumption. As a proof of concept, we applied this protocol in hyperthyroid mice compared to control mice. Hyperthyroidism was induced by chronic treatment with L-thyroxin. This treatment is known to dramatically affect consumption rate of muscle cells.

Results

Typical evolutions of pO2 during breathing challenges are show in fig.1 and 2. Thyroid status significantly modified the muscle oxygen consumption: muscle cells from hyperthyroid mice consumed oxygen faster than muscular cells from control mice (Fig.3).

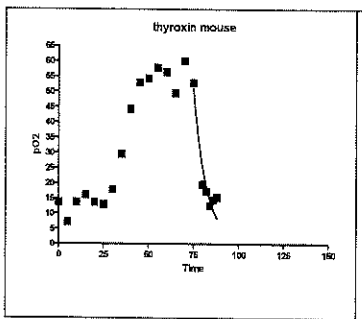

Fig.1: Breathing challenge in hyperthyroid mice.

25 min: air → carbogen
75 min: carbogen → air

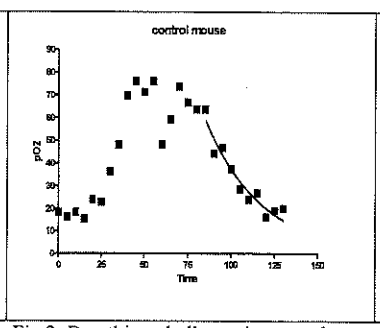

Fig.2: Breathing challenge in control mice.

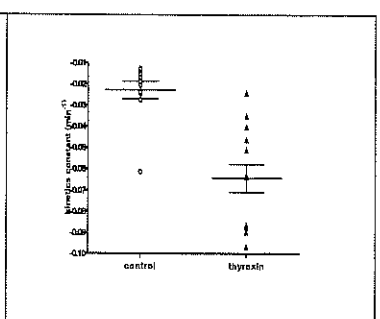

Fig.3: Kinetics constants measured in vivo. Note the faster oxygen consumption by hyperthyroid mic

Bibliography

1. Jordan BF, et al. Insulin increases the sensitivity of tumors to irradiation: involvement of an increase in tumor oxygenation mediated by a nitric oxide-dependent decrease of tumor cells oxygen consumption. Cancer Res. 2002;62/3555-61.

HIGH RESOLUTION 2D AND 3D EPR IMAGING OF MELANIN IN INSECTS

E.S.Vanea, N. Charlier, M. Dinguizli, and B. Gallez

Laboratory of Biomedical Magnetic Resonance, Avenue Mounier 73, Université Catholique de Louvain, B-1200 Brussels, Belgium

Purpose

Electron paramagnetic resonance (EPR) imaging can be described as the spatial and spectral distribution of EPR signals arising from paramagnetic species, in one to three spatial dimensions, using appropriate magnetic field gradients. Melanins are polymeric pigments that contain several free radical centres. At room temperature, the organic semiquinone-type free radical presents a single line (g value of 2.003 to 2.005), with a line width of 5 to 10 Gauss, depending on the melanin type or environment. These features made these free radicals potential candidates for detection and mapping by EPR. To illustrate this approach, we conducted EPR experiments and we looked to the distribution of chitin-melanin and melano-protein complexes in different kinds of insects (bees, ladybirds, woodlouses, scarabs).

Methods and Materials

The collected insects were freeze-dried. A variety of spatial and spectral-spatial EPR imaging were carried out at room temperature using instrumentation consisting of Bruker ELEXSYS equipped with a Super High Sensitivity Probe in combination with a super X bridge (9.85 GHz).

Results

Illustrative images of the distribution of melanin radicals are presented below (Fig 1, Fig 2, Fig 3). 3D EPR image revealed that the melanin was present in the cuticle of the insects (chitin-melanin complexes). Besides these free radicals contained in chitin, areas rich in melanin were observed in other locations, such as the optical lobes of bee's brain.

Conclusions

EPR imaging can provide unique information concerning the spatial distribution of the melanin free radicals in biological samples. In natural sciences, this technique could provide detailed information on the areas that are rich in melanin in insects, and may provide a way to characterize the influence of environmental factors (such as insecticides) on the carapace of insects.

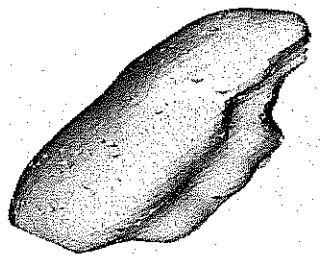

Fig 1.
3D EPRI of scarab's body

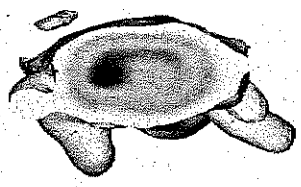

Fig 2.
3D EPRI, section of bee's head

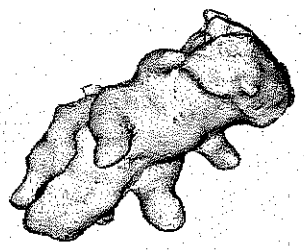

Fig 3.
3D EPRI of bee's body

EVALUATION OF DOSE DISTRIBUTION IN LITHIUM FORMATE PELLETS USING EPRI

E.S.Vanea, J-M. Denis, S. Vynckier, and B. Gallez

Laboratory of Biomedical Magnetic Resonance, Avenue Mounier 73, Université Catholique de Louvain, B-1200 Brussels, Belgium

Purpose

Electron Paramagnetic Resonance (EPR) spectroscopy has been successfully applied to determine radiation dose by using alanine as a radiation–sensitive material: the EPR signal intensity directly reflects the number of stable free radicals produced in solid matrix, and provides a quantitative measurement of the absorbed dose. Here, we hypothesized that this principle can be extended by using EPR Imaging in order to provide convenient information on the spatial dose distribution. For that purpose, we selected lithium formate as a dosimetric material. Compared to alanine, lithium formate possess a high stability, is tissue equivalent and shows a sensitivity much higher than alanine (E. Lund et al., 2005). Moreover, the irradiated lithium formate presents a single EPR line which is particularly convenient for imaging purpose. As a proof of concept, we developed cylindrical tablets of lithium formate, and evaluated by EPR imaging the distribution of free radicals after irradiation by X-Rays or by brachytherapy implants.

Methods and materials

Samples of polycrystalline lithium formate monohydrate were made in the form of cylindrical pellets with a manual pellet press. Some pellets were external irradiated using an X ray beam (250 kV) having a lead protection in order to visualize the different non-irradiated shapes. For brachytherapy studies, pellets with one hole in the middle and with 2 holes were prepared in order to introduce the ^{125}I and ^{192}Ir radioactive sources. The EPR images were acquired using an EPR Elexsys E540 system, operating at 1.1 GHz.

Results

Fig. 1 shows a pellet which was homogeneously irradiated. Fig. 2 shows an EPR image received on a pellet where a lead plate (triangle shape) was partly covering the surface. In Fig. 3, the image was obtained on a pellet irradiated in the centre by a brachytherapy ^{192} Ir wire. Fig. 4 represents the dose distribution around two ^{125}I radioactive seeds. The color code directly reflects the gradient of dose received by using this radioactive material.

Conclusions

Lithium format pellets represent a new modality to assess, by EPRI, the gradient of dose distribution after irradiation. This method offers unique spatial information, especially for the study of dosimetry around brachytherapy seeds.

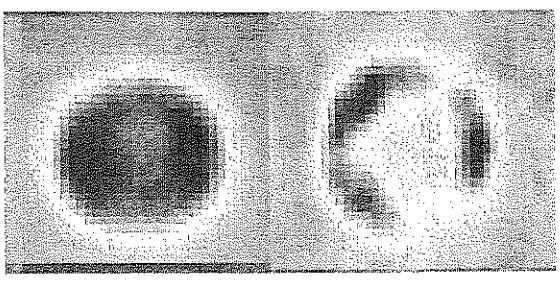

Fig. 1
Homogeneously irradiated lithium formate pellet

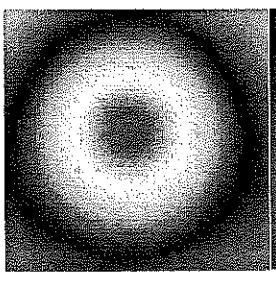

Fig. 2
Lithium formate pellet irradiated with triangle lead protection

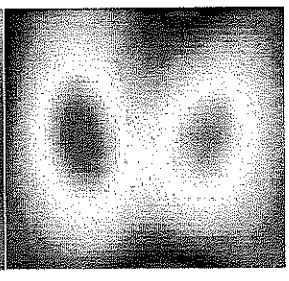

Fig. 3
Lithium formate pellet irradiated in the centre by an ^{192} Ir wire

Fig. 4
Two holes lithium formate pellet irradiated with two ^{125}I radioactive seeds

PHARMACOKINETICS OF DIFFERENT USPIO TYPES DETERMINED BY EPR SPECTROSCOPY

K.A. Radermacher, N. Beghein, B. Gallez
Laboratory of Biomedical Magnetic Resonance, Avenue Mounier 73, Université Catholique de Louvain, B-1200 Brussels, Belgium

Aim of the study:
Iron oxide nanoparticles possess superparamagnetic properties and are used as negative MRI contrast agent by reducing T_2 and T_2^*. The distribution of these iron oxide particles can be monitored by their effect on NMR relaxation times. Besides this method, EPR offers the possibility of a sensitive and quantitative determination of these particles as previously demonstrated by Iannone er al.
Since that time, many different USPIO preparations have been developed. Moreover, USPIO are also used to label stem cells as well as in attempts of molecular imaging using convenient coating that should target them to selective receptors.
Our purpose is to evaluate the value of EPR as a quantitative method to determine the biodistribution of several kinds of USPIO.

Methods and Materials:
We established a calibration curve for different ferrite types (Resovist®, Endorem®, Sinerem®). These particles differ in size and coating. The biodistribution of these products was evaluated in mice by collecting blood, liver and spleen. The concentration of USPIO was determined by an EPR X-band (Bruker, EMX, 9.5 GHz).

Results:
The EPR spectra of the different iron oxide particles are quite different from each other because of the different sizes and coatings. In general, a very broad line (500 to 1000 G) was observed with a center field near to 3350 G. Typical distributions are shown in Fig. 1 and 2. For Resovist, we can observe a very quick decrease of the iron concentration in blood, whereas the contrast agent was quickly taken up in the liver and spleen. The concentrations remains constant up to 24h. Now we are evaluating the distribution of targeted USPIO in normal and pathological models.

Reference: Iannone et al. Investigative Radiology, June 1992, Vol.27, No.6, 450-455.

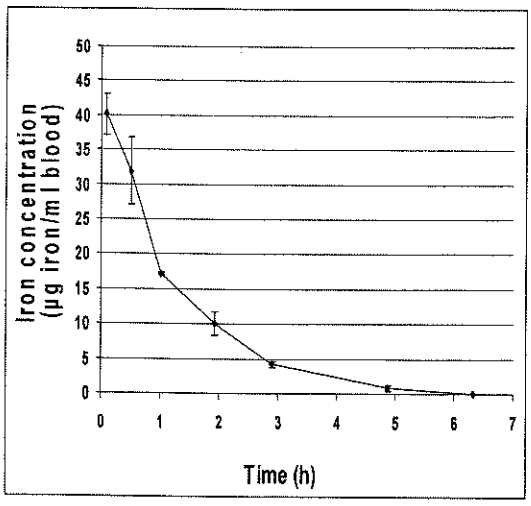

Fig.1: Kinetics curve of Resovist® in blood.

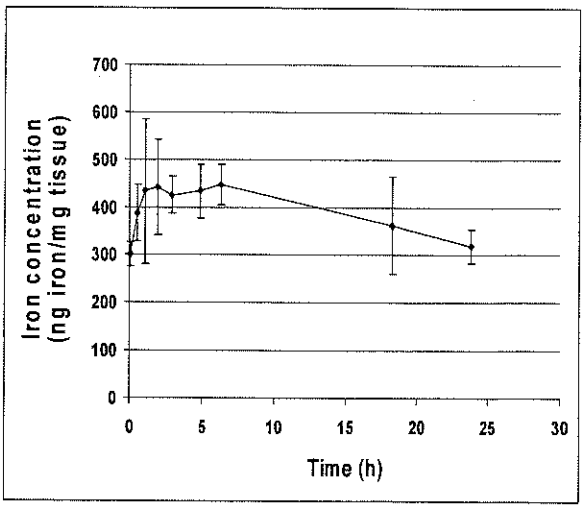

Fig.2: Kinetics curve of Resovist® in the liver.

WHAT IS THE REAL PO_2 IN THE SUBCUTANEOUS TISSUE?

M. Dinguizli, N. Beghein, and B. Gallez

Laboratory of Biomedical Magnetic Resonance, Avenue Mounier 73, Université Catholique de Louvain, B-1200 Brussels, Belgium

Introduction:

Different methods can be used to measure oxygen in the subcutaneous tissue. EPR oximetry using implantable carbon materials has been used both in animals and in pionneer human studies carried out in Dartmouth Medical School. Surprinsingly, these EPR studies indicate an apparent low pO_2 (10 mm Hg) in the SC tissue. These results are in contradiction with those values obtained so far with invasive methods such as oxygen electrodes used in several studies (1).Considering these opposite results, we tried to clarify this point using sequential monitoring of pO_2 using EPR oximetry and OxyLite probes.

Materials and Methods:

Sensors (Charcoal and Carbon black suspension 100mg/ml) were injected intradermically (5*10µl) or in the subcutaneous tissues (50µl) of the leg (NMRI mice).at least 2 weeks before EPR measurement.

Under anesthetia by isoflurane, the pO_2 was measured by two techniques : EPR oximetry with a 1.2 GHz spectrometer and OxyLite system. Localization and biocompatibility were systematically verified by histology. pO_2 were measured by EPR just before and just after OxyLite. pO_2 measurement by OxyLite was started after one hour equilibrium and the body temperature was controlled and stabilized at 36°C. (Fig 2)

Results:

Initial pO_2 measurements by EPR oximetry show very low values in subcutaneous area (10 mm Hg). Those values have been confirmed by complementary experiments where the pO_2 in the SC tissue was measured over the time (60 days (Fig 3). After the insertion of the OxyLite probes, the pO_2 recording using this system indicate significant larger values (around 40 mm Hg). Immediately after the OxyLite measurements, EPR oximetry was again used. The second EPR measurements indicate systematically pO_2 increased compared to the first measurement (Fig1) .

Discussion:

A provocative explanation of this set of experiments is that the use of invasive methods could not be suitable for measurement of pO_2 in SC tissue. All EPR results obtained so far (with different oxygen sensors) are consistent with a very low vascularization of this tissue, with a pO_2 dramatically lower than in the well vascularized derma. When inserting a probe in a tissue which is very closed to the aerated surface of the skin, the pO_2 measured could be influenced by the track made with the needle. This may explain the high pO_2 values recorded after this insertion using both methods.

Conclusion:

While comparison of oximetry methods are generally valuable in deep tissues, the use of invasive methods near the skin potentially disturb the local pO2.

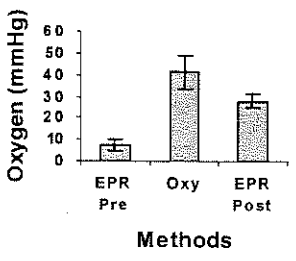

Fig 1 : Sequential monitoring of pO_2 using EPR oximetry and OxyLite probes.

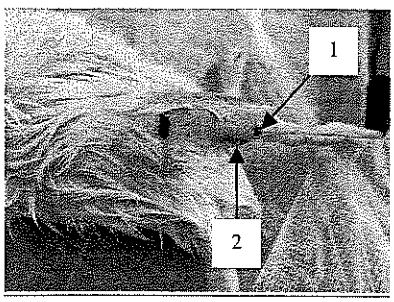

Fig 2 : Sites of probes implantation in mice: **1** probe for EPR; **2** site of introduction of OxyLite

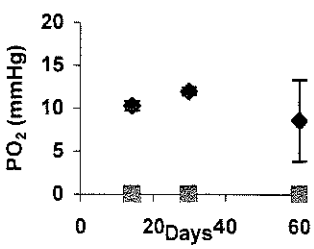

Fig 3 : pO_2 monitoring over the time in subcutaneous area before (blue) or after (rose) ligation of the leg.

RETRIEVABLE MICRO-PELLETS FOR MONITORING TISSUE OXYGEN PRESSURE

Dinguizli M, Beghein N and Gallez B

Laboratory of Biomedical Magnetic Resonance, Avenue Mounier 73, Université Catholique de Louvain, B-1200 Brussels, Belgium

Introduction

The evolution of the oxygen pressure in tissues is a crucial information in physiology, pathophysiology and therapy such as radiation oncology. EPR oximetry is based on the introduction of an oxygen sensor in tissues. By measuring the EPR line width which is very sensitive to the oxygen environment, it is possible to measure oxygen from the same site over long periods of time.

Objectives

The present study deals with the development of biocompatible and retrievable inserts that may be used in EPR oximetry. Here, we developed and evaluated cylindrical micro-pellets made of Teflon holding lithium phthalocyanine (LiPc) as oxygen sensors. This configuration should enable to protect the tissues from direct interactions with the sensor. Moreover, the design was chosen to allow an easy implantation in tissues, to avoid a spreading of the sensors inside the tissues, and to allow the removal of the sensor after use. Two types of applications are sought: 1) use in animal in very precise areas (such as brain studies in animals); 2) first use in clinical EPR oximetry

Materials and Methods

Cylindrical micro-pellets were made by injection into a Teflon® AF2400 tubing (ID: 0.034") of a suspension of LiPc in a solution of Teflon® AF2400 in FC-75 solvent (3% p/v). The pellets were then dried for 24 h in an oven at 70°C. X Band EPR was used to build calibration curves and to determine the kinetics of response of the sensor (EPR line width as a function of pO2). Micro-pellets were sterilized by dry heating (120°C for 24 hours). Micro-pellets were surgically implanted in muscles and subcutaneous areas of the leg of mice. A L-Band EPR spectrometer was used to determine the oxygen pressure *in vivo*.

Results

Using the described procedure, it was possible to develop micro-pellets with different sizes (Figure 1). LiPc crystals were homogenously distributed in the cylinder. Optical verification of micro-implants allow to select micro-pellets without bubbles or cracks. The kinetics response of the sensor was very rapid when changing the oxygen environment of the sensor (Figure 2). *In vivo* studies in subcutaneous area gave pO_2 values stable over the time (42 days), (Figure 3).

Conclusions

Micro-retrievable inserts holding EPR oxygen sensors have been developed. The new design allows the preservation of the favorable characteristics of LiPc, while allowing easy implantation inside the tissues and removal from the tissues after studies. This design could be valuable for first clinical EPR oximetry studies in patients.

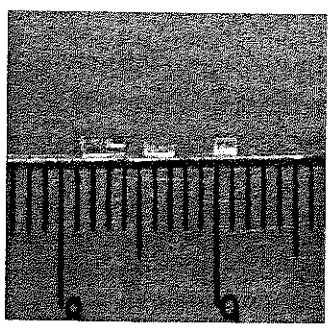

Figure 1 : Picture of micro-pellets holding LiPc crystals

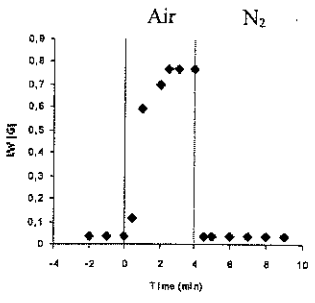

Figure 2 : Response of the LiPc inserted in the micro-pellets to changes in oxygenation in the environment

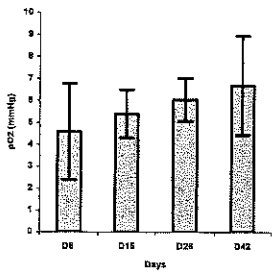

Figure 3: *In vivo* EPR measurements carried out in the subcutaneous area in mice .

CHARACTERIZATION OF SELF-ASSEMBLING COPOLYMERS IN AQUEOUS SOLUTIONS USING EPR AND FLUORESCENCE SPECTROSCOPY.

N. Beghein, L. Rouxhet, M. Dinguizli, M. Brewster, A. Arien, V. Préat, J.L. Habib and Bernard Gallez

Laboratory of Biomedical Magnetic Resonance, Avenue Mounier 73, Université Catholique de Louvain, B-1200 Brussels, Belgium

Purpose

Polymeric micelles are formed by the self-assembly of block amphiphilic copolymers. They can be used to solubilize poorly soluble drugs. In order to optimize the use of self-assembling copolymers, there is a clear need for a better characterization of the local microviscosity and micropolarity gradient. This information could eventually lead to a better representation of their structure.
EPR (9.3GHz) and fluorescence spectroscopy have been used to determine the micropolarity and microviscosity of self-assembling systems based on mmePEG-p(CL-co-TMC) having different PEG chain lengths and different CL/TMC ratios and PEG/MOG/SA (45/5/50) polymers with different PEG chain lengths. Four different reporter probes have been used: two spin probes, 16-doxyl stearic acid and 5-doxylstearic acid, and two fluorescent probes, pyrene and 1,3-bis(1-pyrenyl) propane (P3P).

Methods and Materials

The polymers of interest were the polymers made of monomethoxylated polyethylene glycol (mmePEG), caprolactone (CL) and trimethylene carbonate (TMC), mmePEG-p(CL-co-TMC), with different CL/TMC ratios (30/70, 50/50, 70/30) and PEG chain lengths (750 and 2000 Da) and the polymers made of 45 mol% polyethylene glycol (PEG), 5 mol% monooleyl glycerol (MOG) and 50 mol% succinic anhydride (SA), PEG/MOG/SA (5/45/50), with different PEG chain lengths (400, 600, 1000 Da).

Results and conclusion

We found that the micelles with mmePEG-p(CL-co-TMC) polymers are of a biphasic nature. The micelles are made of a hydrophilic corona with low viscosity while the core of the micelle is more hydrophobic and more viscous. The outer shell would be made of PEG chains, the hydrophobic part of the chains making the core. The partial hydration of the shell seems to lead to a looser chains network than deeper in the micelles. By contrast, in micelles with PEG/MOG/SA, there is no clear domain separation. This is consistent with a spatial configuration of random polymeric chains forming a loose network. In these micelles, the microviscosity is low and the hydrophobicity is high

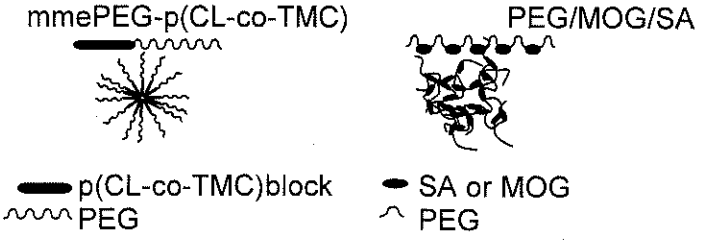

Participants

Aguirre, Aranzazu, Department of Physics, University of Antwerp – UIA, Universiteitsplein 1, B - 2610 Wilrijk, Belgium, aranzazu.aguirre@ua.ac.be

Bruin, Bas de, van 't Hoff Institue for Molecular Sciences, Department of Homogenous Catalysis, HIMS, Univ. Of Amsterdam, Nieuwe Achtergracht 166, 1018 WV Amsterdam, The Netherlands, tel: +31-205256495; bdebruin@science.uva.nl.

Callens, Freddy, Universiteit Gent, Dept Solid State Sciences, Krijgslaan 281, S1, B-9000 Gent, Belgium; freddy.callens@ugent.be

Cambre, Sofie, Department of Physics, University of Antwerp – UIA, Universiteitsplein 1, B - 2610 Wilrijk, Belgium, Tel: +32 3820 2482; sofie.cambre@ua.ac.be

Caretti, Ignatio, Department of Physics, University of Antwerp – UIA, Universiteitsplein 1, B - 2610 Wilrijk, Belgium, Tel: +32 3820 2479; ignatio.caretti@ua.ac.be.

Charlier, Nicolas, Catholic University of Louvain, Lab. Chem. Med, Avenue Mounier 73. 40, B-1200 Brussels, Belgium

Clémer, Katrijn, Department of Physics, University of Leuven, Celestijnenlaan 200D, 3001 Leuven, Belgium; katrijn.clemer@fys.kuleuven.ac.be.

Desmet, Filip, Department of Physics, University of Antwerp – UIA, Universiteitsplein 1, B - 2610 Wilrijk, Belgium; **filip.desmet@ua.ac.be**.

Diepart, Caroline, Catholic University of Louvain, Lab. Chem. Med, Avenue Mounier 73. 40, B-1200 Brussels, Belgium

Doorslaer, Sabine van, Department of Physics, University of Antwerp – UIA, Universiteitsplein 1, B - 2610 Wilrijk-Antwerpen, Belgium; sabine.vandoorslaer@ua.ac.be.

Dzik, Wojciech, Department of Homogenous Catalysis, HIMS, Univ. Of Amsterdam, Nieuwe Achtergracht 166, 1018 WV Amsterdam, The Netherlands; dzik@science.uva.nl.

Ezhevskaya, Maria A. Department of Physics, University of Antwerp – UIA, Universiteitsplein 1, B - 2610 Wilrijk, Belgium; maria.ezhevkaya@ua.ac.be.

Faassen, Ernst van, Faculty of Science, section Interface Physics, Ornstein laboratory, Utrecht university, 3508 TA Utrecht, The Netherlands; e.e.h.vanfaassen@phys.uu.nl.

Gallez, Bernard, Catholic University of Louvain, Lab. Chem. Med, Avenue Mounier 73. 40, B-1200 Brussels, Belgium; tel: 02 764 2789, gallez@cmfa.ucl.ac.be

Gast, Peter, Leiden Inst. Physics, University of Leiden, PO Box 9405, 2300 RA Leiden, The Netherlands; tel:+31-715275979; fax:+31-71-5275819; gast@molphys.leidenuniv.nl.

Goovaerts, Etienne, Department of Physics, University of Antwerp – UIA, Universiteitsplein 1, B - 2610 Wilrijk, Belgium; Tel: +32 3820 2446, Fax +32-3820 2470, Etienne.goovaerts@ua.ac.be

Groenen, Edgar.J.J., Leiden Inst. Physics, University of Leiden, PO Box 9405, 2300 RA Leiden, The Netherlands; tel:+31-715275914; fax:+31-71-5275819; egroenen@molphys.leidenuniv.nl

Hagedoorn, Peter L., Delft University of Technology, Department of Biotechnology, Julianalaan 67, 2628 BC Delft, The Netherlands pl.hagedoorn@tudelft.nl.

Hoff, Ton van 't, BRUKER BioSpin BV PO Box 88, 1530 AB Wormer, The Netherlands; tel: +31-75-6285251; fax:+31-75-6289771; a.n.vanthoff@bruker.nl.

Huber, Martina I., Leiden Inst. Physics, University of Leiden, PO Box 9405, 2300 RA Leiden, The Netherlands; tel:+31-715275560; fax:+31-71-5275819; mhuber@molphys.leidenuniv.nl

Ijaz, Ahmad, Department of Physics CDE, University of Antwerp – UIA, Universiteitsplein 1, B - 2610 Wilrijk-Antwerpen, Belgium.

Ioanitescu, Iulia, SIBAC Laboratory. Department of Physics, University of Antwerp – UIA, Universiteitsplein 1, B - 2610 Wilrijk, Belgium,

Jivanescu, Mihaela, Department of Physics, University of Leuven, Celestijnenlaan 200D, 3001 Leuven, Belgium; mihalea.jivanescu@fys.kuleuven.ac.be.

Keunen, Koen, Department of Physics, University of Leuven, Celestijnenlaan 200D, 3001 Leuven, Belgium; koen.keunen@fys.kuleuven.ac.be.

Lobysheva , Irina, Unit of Pharmacology and Therapeutics, University of Louvain Medical School, 53, Avenue Mounier, FATH 5349/ U.C.L..1200 Brussels, Belgium; irina.lobysheva@mint.ucl.ac.be.

Milikisyant, Sergey, Leiden Inst. Physics, University of Leiden, PO Box 9405, 2300 RA Leiden, The Netherlands, tel:+31-715275912; fax:+31-71-5275819.

Moons, Hans, Department of Physics CDE, University of Antwerp – UIA, Universiteitsplein 1, B - 2610 Wilrijk-Antwerpen, Belgium,

Nagy, Nora V., Department of Physics, University of Antwerp – UIA, Universiteitsplein 1, B - 2610 Wilrijk-Antewerpen, Belgium, nora.nagy@ua.ac.be.

Nistor, Sergiu V., National Institute for material Physics, Atomistilor 105bis Street, PO Box MG 7 Magurele RO 077125 Bucharest, Romania, tel: +40-214930195; fax: +40-214930267; snistor@infim.ro.

Radermacher, Kim, Catholic University of Louvain, Lab. Chem. Med, Avenue Mounier 73. 40, B-1200 Brussels, Belgium.

Rath, J.K. SID University of Utrecht, Physics of devices, RvdG laboratory, PO Box 80000 3508 TA Utrecht; The Netherlands; tel: +31-302532961; fax: +31-032543165, j.k.rath@phys.uu.nl

Scarpelli, Francesco, Leiden Inst. Physics, University of Leiden, PO Box 9405, 2300 RA Leiden, The Netherlands; tel:+31-715275908; fax:+31-71-5275819; scarpelli@molphys.leidenuniv.nl

Shamuilia, Sheron, Department of Physics , University of Leuven, Celestijnenlaan 200D, 3001 Leuven, Belgium, sheron.shamuilia@fys.kuleuven.ac.be.

Somers, Pieter, Department of Physics, University of Leuven, Celestijnenlaan 200D, 3001 Leuven, Belgium, pieter.somers@fys.kuleuven.be.

Sottini, Silvia, Leiden Inst. Physics, University of Leiden, PO Box 9405, 2300 RA Leiden, The Netherlands, tel: +31-715275908; fax: +31-71-5275819; sottini@molphys.leidenuniv.nl.

Stefan, Mariana, National Institute for material Physics, Atomistilor 105bis Street, PO Box MG 7 Magurele RO 077125 Bucharest, Romania , tel: +40-214930195; fax: +40-214930267; mstefan@infim.ro.

Stesman Andre, Department of Physics, University of Leuven, Celestijnenlaan 200D, 3001 Leuven, Belgium, andre.stesman@fys.kuleuven.ac.be.

Trandafir, Florin, Department of Physics, University of Antwerp – UIA, Universiteitsplein 1, B - 2610 Wilrijk, Belgium, florin.trandafir@ua.ac.be.

Vanea, Emilia, Catholic University of Louvain, Lab. Chem. Med, Avenue Mounier 73. 40, B-1200 Brussels, Belgium.

Vinck, Evi, Department of Physics, University of Antwerp – UIA, Universiteitsplein 1, B - 2610 Wilrijk, Belgium, Tel: +32-3820-2482, evi.vinck@ua.ac.be

Vrielinck, Henk, Dept. Solid State Science; Ghent University, Krijgslaan 281-S1, B-9000 Gent, Belgium, henk.vrielinck@rug.ac.be

Zamani, Sepideh, Department of Physics, University of Antwerp – UIA, Universiteitsplein 1, B - 2610 Wilrijk, Belgium, sepideh.zamani@ua.ac.be.

Zverev, Dimitry, Universiteit Gent, Dept Solid State Sciences, Krijgslaan 281, S1, B-9000 Gent, Belgium.